



HAL
open science

Store-Operated Calcium Entries Control Neural Stem Cell Self-Renewal in the Adult Brain Subventricular Zone

Florence Domenichini, Elodie Terrié, Patricia Arnault, Thomas Harnois, Christophe Magaud, Patrick Bois, Bruno Constantin, Valérie Coronas

► **To cite this version:**

Florence Domenichini, Elodie Terrié, Patricia Arnault, Thomas Harnois, Christophe Magaud, et al.. Store-Operated Calcium Entries Control Neural Stem Cell Self-Renewal in the Adult Brain Subventricular Zone. *STEM CELLS*, 2018, 36 (5), pp.761-774. 10.1002/stem.2786 . hal-01705161

HAL Id: hal-01705161

<https://hal.science/hal-01705161>

Submitted on 18 Nov 2022


HAL is a multi-disciplinary open access archive for the deposit and dissemination of scientific research documents, whether they are published or not. The documents may come from teaching and research institutions in France or abroad, or from public or private research centers.

L'archive ouverte pluridisciplinaire **HAL**, est destinée au dépôt et à la diffusion de documents scientifiques de niveau recherche, publiés ou non, émanant des établissements d'enseignement et de recherche français ou étrangers, des laboratoires publics ou privés.



Distributed under a Creative Commons Attribution - NonCommercial - NoDerivatives 4.0 International License

Store-Operated Calcium Entries Control Neural Stem Cell Self-Renewal in the Adult Brain Subventricular Zone

FLORENCE DOMENICHINI,* ELODIE TERRIÉ,* PATRICIA ARNAULT, THOMAS HARNOIS, CHRISTOPHE MAGAUD, PATRICK BOIS, BRUNO CONSTANTIN, VALÉRIE CORONAS 

Key Words. Adult stem cells • Calcium flux • Nervous system • Neural stem cell • Self-renewal • Stem cell asymmetry • Stem cell–microenvironment interactions • Stem cells • Neurogenesis/neural regeneration • Stem cell niche

Signalisation et Transports Ioniques Membranaires, University of Poitiers, CNRS ERL 7003, Poitiers Cedex 09, France

*Co-first authors.

Correspondence: Valérie Coronas, Ph.D., Signalisation et Transports Ioniques Membranaires, University of Poitiers, CNRS ERL 7003, Bat B36, 1 rue Georges Bonnet-TSA 51 106, 86073 Poitiers Cedex 09, France. Telephone: 33 (0)5 49 45 36 55; e-mail: valerie.coronas@univ-poitiers.fr

Received July 20, 2017; accepted for publication January 10, 2018; first published online in *STEM CELLS EXPRESS* January 23, 2018.

<http://dx.doi.org/10.1002/stem.2786>

ABSTRACT

The subventricular zone (SVZ) is the major stem cell niche in the brain of adult mammals. Within this region, neural stem cells (NSC) proliferate, self-renew and give birth to neurons and glial cells. Previous studies underlined enrichment in calcium signaling-related transcripts in adult NSC. Because of their ability to mobilize sustained calcium influxes in response to a wide range of extracellular factors, store-operated channels (SOC) appear to be, among calcium channels, relevant candidates to induce calcium signaling in NSC whose cellular activities are continuously adapted to physiological signals from the microenvironment. By Reverse Transcription Polymerase Chain Reaction (RT-PCR), Western blotting and immunocytochemistry experiments, we demonstrate that SVZ cells express molecular actors known to build up SOC, namely transient receptor potential canonical 1 (TRPC1) and Orai1, as well as their activator stromal interaction molecule 1 (STIM1). Calcium imaging reveals that SVZ cells display store-operated calcium entries. Pharmacological blockade of SOC with SKF-96365 or YM-58483 (also called BTP2) decreases proliferation, impairs self-renewal by shifting the type of SVZ stem cell division from symmetric proliferative to asymmetric, thereby reducing the stem cell population. Brain section immunostainings show that TRPC1, Orai1, and STIM1 are expressed *in vivo*, in SOX2-positive SVZ NSC. Injection of SKF-96365 in brain lateral ventricle diminishes SVZ cell proliferation and reduces the ability of SVZ cells to form neurospheres *in vitro*. The present study combining *in vitro* and *in vivo* approaches uncovers a major role for SOC in the control of SVZ NSC population and opens new fields of investigation for stem cell biology in health and disease. *STEM CELLS* 2018; 00:000–000

SIGNIFICANCE STATEMENT

The present study addresses the roles in adult neural stem cells (NSC) of store-operated channels (SOC), which are calcium channels that have the capacity to mobilize calcium influxes in response to a wide range of extracellular signals. Our study combining multiple *in vitro* and *in vivo* approaches, demonstrates that NSC express SOC that support calcium entries (SOCE), and that pharmacological inhibition of SOCE decreases proliferation and self-renewal of NSC by promoting asymmetric at the expense of symmetric proliferative division. Our study opens new perspectives for examining further the physiological roles of SOC within stem cells and their involvement in brain physiopathology.

INTRODUCTION

Stem cells contribute to homeostasis and repair of the tissues wherein they reside by providing new differentiated cells. In the brain of adult rodents, the subventricular zone (SVZ) bordering lateral ventricles is the major reservoir of neural stem cells (NSC) [1]. Within the murine SVZ germinal niche, NSC proliferate, self-renew and continuously provide thousands

of olfactory bulb neurons every day, as well as a small number of myelinating oligodendrocytes [2–5]. Recruited by injuries, NSC contribute to brain repair and consequently, to functional recovery [6–10]. Cells that proliferate *in vivo* and that behave as multipotent progenitor cells *in vitro* have also been found in the lateral ventricle walls of the human brain [11, 12]. These human SVZ stem cells could even be harvested by endoscopy for *in*

in vitro expansion [13]. Although the ability of SVZ cells to sustain neurogenesis in healthy human brain in vivo is debated and seems limited to striatum for neuronal production, several reports support that as in rodents, SVZ cells are recruited and generate neuroblasts in the injured human brain after an ischemic stroke [14–20]. This capacity is retained even in old age [21]. Taking into account the considerable hope that discovery of NSC has nurtured for brain repair, there is an urgent need for understanding the mechanisms that govern NSC, which is a prerequisite for the manipulation of adult stem cells and neurogenesis.

Previous transcriptome studies underlined enrichment in transcripts related to calcium signaling in NSC in both mice and humans [22, 23]. Calcium is a ubiquitous second messenger whose oscillations of its cytosolic concentration are used as a key signal in virtually every mammalian cell [24]. Changes in cytosolic calcium levels are consecutive to either a release from intracellular calcium stores or a calcium influx from the extracellular medium through calcium channels of the plasma membrane. In many cell types, store-operated calcium entry (SOCE) is an important pathway for calcium influx from the extracellular space. Activated by emptying of intracellular calcium stores, among which the most important reservoir is the endoplasmic reticulum (ER), SOCE occurs through store-operated channels (SOC) that are mainly formed of Orai1 and also of transient receptor potential canonical (TRPC1) [25, 26]. SOCE is coordinated by stromal interaction molecule 1 (STIM1) protein from the ER that acts as an ER calcium sensor and activates SOC (see Graphical abstract). SOCE is triggered after G protein-coupled or tyrosine kinase-coupled receptors, acting through phospholipase C (PLC)/inositol triphosphate (IP3) pathway, stimulate the release of calcium from the ER stores via IP3 receptor. The subsequent reduction of calcium content in the ER is sensed by STIM1 that oligomerizes and in turn, activates SOC thereby inducing a calcium entry. This SOCE not only allows refilling of calcium stores, but also evokes a sustained calcium signal that drives a wide range of cellular and physiological effects.

SOC are involved in pleiotropic cell functions including proliferation of endothelial cells or lymphocytes, motility of keratinocytes as well as migration of mesenchymal stem cells or myoblasts [27–31]. Early evidence for a crucial role of SOC channels in human health came from the analysis of patients with rare inherited immunodeficiency diseases [32]. Consecutive studies on patients or on mice with Orai1 deficiency revealed in addition to severe immune defects, impairments in skeletal development, myopathy and alterations in hair cell function or skin integrity [33–35]. Genetic invalidation of TRPC1 also resulted in major regeneration impairments of damaged muscle or intestinal mucosa [36, 37], pointing to possible roles of SOC in the maintenance of tissue homeostasis.

Along with reports showing a decreased proliferation of neural progenitors following pharmacological or genetic alterations of SOC [38–40], these above data prompted us to conduct the present study aimed at deciphering the involvement of SOC in NSC. By using multiple in vitro and in vivo approaches, we demonstrate that SVZ cells express SOC whose pharmacological inhibition decreases proliferation and self-renewal by promoting asymmetric division at the

expense of symmetric proliferative division of NSC in the SVZ.

MATERIALS AND METHODS

Animals

Experiments were performed on C57BL/6J mice. Animals were housed in PREBIOS facilities for animal care (University of Poitiers). All experimental procedures were carried out in accordance with the guidelines of the French Ministry of Agriculture (decree 87849) and the European Communities Council Directive (2010/63/EU) and validated by the Regional Ethical Committee (Authorization n°02184.01).

Solutions and Chemicals

SKF-96365 and YM-58483 (BTP2) were purchased from Sigma Aldrich (Saint-Louis) and dissolved in water and dimethylsulfoxide (DMSO), respectively. Cell culture media and growth factors were purchased from Invitrogen (Carlsbad, CA).

SVZ Cell Culture

SVZ was microdissected out of C57BL/6J mice brains, dissociated as single cells and grown in DMEM-F12 supplemented with B27 and with 10 ng ml⁻¹ epidermal growth factor (EGF) and 5 ng ml⁻¹ fibroblast growth factor (FGF2) as previously described [41]. Neurospheres obtained after a week in vitro, were dissociated as single cells and seeded to obtain secondary neurospheres that were used for calcium imaging assays, Reverse Transcription Polymerase Chain Reaction (RT-PCR), Western blotting, immunostaining, and cell proliferation assays.

RT-PCR

Total RNA was prepared from SVZ cell cultures using RNable reagent (Eurobio, Les Ulis, France). One microgram of RNA was reverse transcribed at 37°C for 1 hour by using 400U M-MLV Reverse Transcriptase (Invitrogen) and 1.5 µg Random Primer Pd(N)₆ (Invitrogen). PCR reactions were performed using *Taq* polymerase (Invitrogen) and the primers described in Supporting Information Table S1. RNA extracted from C2C12 myoblasts was used as positive controls [42]. Negative control was performed in the absence of RNA template.

Western Blot

For Western blotting analysis, 10⁶ SVZ cells were lysed in Laemmli loading buffer (Sigma Aldrich). Samples were resolved in a 9% gradient SDS-polyacrylamide gel. Proteins were transferred to Amersham Protran nitrocellulose membranes (0.20 µm-pore size; GE Healthcare, Little Chalfont, U.K.). Immunoblots were probed overnight at 4°C in TBS-Tween with 3% fat milk with one of the following antibodies: polyclonal rabbit anti-Orai1 (H-46, Santa Cruz Biotechnology, Dallas, TX; 0.4 µg ml⁻¹), monoclonal mouse anti-STIM1 (GOK 610954, BD Biosciences, Franklin Lakes, NJ; 0.4 µg ml⁻¹), monoclonal mouse anti-TRPC1 (E-6, Santa Cruz Biotechnology; 0.4 µg ml⁻¹) or polyclonal rabbit anti-actin (Sigma Aldrich; 1/5,000) before incubation with anti-mouse or anti-rabbit immunoglobulin-HRP-linked (1/5,000; GE Healthcare) and detection with ECL (Immobilon, Millipore, Billerica, MA). Results were analyzed with GeneGnome XRQ (SYNGENE Ozyme, Cambridge, U.K.).

Immunostaining

For immunostaining of brain sections, mice were deeply anaesthetized and transcardially perfused with a 9 g l^{-1} NaCl solution followed by 4% paraformaldehyde. Brains were removed, post-fixed, and cryoprotected. Frontal brain sections, $40 \mu\text{m}$ thick, were cut using a Leica cryostat and processed for immunohistochemistry.

For immunostaining, SVZ neurospheres were thrown on glass slides with a cytospin and fixed in methanol at -20°C . For immunostaining on single cells, SVZ neurospheres were dissociated, plated on polylysine-coated glass coverslips for 24 hours and fixed.

After permeabilization and blockade of non-specific binding sites, the preparations were stained using one of the antibodies listed in Supporting Information Table S2 and then incubated with the appropriate Alexa fluor 555 or Alexa fluor 488 conjugated antibodies before analysis with a spectral confocal FV-1000 station installed on an inverted microscope IX-81 (Olympus). 4',6-diamidino-2-phénylindole (DAPI) or TOPRO-3 was used to label nuclei. The emitted fluorescence was detected through spectral detection channels between 425–475 nm, 500–530 nm and 550–625 nm, for UV, green and red fluorescence, respectively and through a 650 nm long pass filter for far red fluorescence.

Intracellular Calcium Measurements

Cells were plated at $30,000 \text{ cells ml}^{-1}$ on glass coverslips coated with poly-L-lysine. After 72 hours, cells were incubated for 30 minutes at 37°C with $6 \mu\text{mol l}^{-1}$ of the single-wavelength calcium sensitive probe fluo-8-AM (Santa Cruz Biotechnology). Assays were performed in a standard external buffer solution (130 mmol l^{-1} NaCl, 5.4 mmol l^{-1} KCl, 0.8 mmol l^{-1} MgCl_2 , 10 mmol l^{-1} HEPES, 5.6 mmol l^{-1} D-glucose, pH 7.4). SVZ cells were perfused with the buffer solution containing 0.1 mmol l^{-1} EGTA (Ca^{2+} -free solution). SOCE was triggered with cyclopiazonic acid (CPA) (Sigma Aldrich, $15 \mu\text{mol l}^{-1}$) or carbachol (Sigma Aldrich, $10 \mu\text{mol l}^{-1}$). Fluorescence images were recorded using a Revolution XD Andor multi-point confocal laser microscopy system equipped with a Yokogawa CSU-X1 spinning disk confocal unit and an Andor EMCCD Camera. The multi-point confocal laser microscopy system was based around an inverted microscope (Olympus IX81-ZDC) equipped with a $60\times$ oil objective and with a microscope incubation chamber. Fluorescence signal was collected at 37°C through the control software Fluoview. Fluo-8-AM was excited at 488 nm and the emitted fluorescence was detected at 522 nm. The intensity of fluorescence emission (F) was measured over time in selected regions of interest on several cells of small neurospheres, normalized to basal fluorescence obtained before stimulation (F_0) and expressed as the ratio of $(F-F_0)/F_0$.

Cell Proliferation Assays

SVZ cell proliferation was evaluated by bromodeoxyuridine (BrdU) incorporation in DNA using an ELISA assay. SVZ neurospheres dissociated as single cells were plated at the concentration of $30,000 \text{ cells ml}^{-1}$ in polylysine-coated 96 well plates and treated for 24 hours with SKF-96365 or YM-58483. BrdU was added to the medium for the last 4 hours of the assay before quantification of BrdU incorporated in DNA according to manufacturer's instructions (Roche diagnostics, Meylan, France).

Cell Culture Growth Assays

SVZ cell culture growth was measured on SVZ neurospheres maintained for 5 days in their culture medium alone (control of SKF-96365), or supplemented with either SKF-96365 ($1 \mu\text{mol l}^{-1}$), or YM-58483 ($5 \mu\text{mol l}^{-1}$), or DMSO (control of YM-58483). The viable cells were counted using the Trypan blue exclusion assay.

Cell Death Assays

SVZ neurospheres dissociated as single cells were plated at the concentration of $100,000 \text{ cells ml}^{-1}$ in 12-well plates and treated for 24 hours with SKF-96365 or YM-58483 at the indicated concentrations. Apoptotic cells were labeled with FITC-conjugated AnnexinV (BD Biosciences) and subjected to FACS analysis (BD FACS verse).

Neurosphere Forming and Self-Renewal Assays

SVZ dissected out of mice brains was dissociated and seeded at $10 \text{ cells } \mu\text{l}^{-1}$ in 24 well plates in the cell culture medium alone or supplemented with either SKF-96365 ($1 \mu\text{mol l}^{-1}$), or YM-58483 ($5 \mu\text{mol l}^{-1}$), or DMSO. After a 7-day incubation period, primary neurospheres were counted under the microscope. For self-renewal assays, neurospheres were collected, centrifuged, and reseeded ($5 \text{ cells } \mu\text{l}^{-1}$) in the culture medium to obtain secondary neurospheres.

SVZ cells obtained and treated as above were also subjected to a neural-colony forming cell assay as described previously [43].

Cell Pair Assays

SVZ dissected out of mice brains was dissociated, plated on polylysine-coated glass coverslips at $10 \text{ cells } \mu\text{l}^{-1}$ and incubated for 18 hours in culture medium containing low concentrations of growth factor (5 ng ml^{-1} EGF and 2.5 ng ml^{-1} FGF2) alone or supplemented with either SKF-96365 ($1 \mu\text{mol l}^{-1}$), or YM-58483 ($5 \mu\text{mol l}^{-1}$), or DMSO. The preparations were then fixed and immunostained for SOX2 and α -tubulin. Cell pairs were analyzed with a spectral confocal FV-1000 station installed on an inverted microscope IX-81 (Olympus).

Cell Differentiation Assays

SVZ neurospheres were dissociated as single cells, plated at the concentration of $80,000 \text{ cells ml}^{-1}$ on polylysine-coated glass coverslips and allowed to adhere to the substrate overnight. SVZ cells were then treated with SKF-96365 ($1 \mu\text{mol l}^{-1}$), or YM-58483 ($5 \mu\text{mol l}^{-1}$), or DMSO for 1 week in culture medium without growth factors. The cultures were then fixed and immunostained for Glial fibrillary acidic protein (GFAP), O4, β III-tubulin, or doublecortin (DCX).

In Vivo Injection of SOC Inhibitors

Two to three months-old mice were anesthetized with 100 mg kg^{-1} ketamine and 10 mg kg^{-1} xylazine. Two microliters of a 9 mg ml^{-1} NaCl solution containing either $100 \text{ ng } \mu\text{l}^{-1}$ EGF or $100 \text{ ng } \mu\text{l}^{-1}$ EGF combined with $6 \text{ nmol } \mu\text{l}^{-1}$ SKF-96365 were injected as a single dose in the left lateral cerebral ventricle using a $5 \mu\text{l}$ Hamilton syringe at the following coordinates [anterior relative to Bregma, lateral, depth below the dura]: 0.74 mm, 0.6 mm, 2.18 mm. Seventy two hours post-intracerebroventricular injections, SVZ was microdissected and subjected to the neurosphere assay.

For the analysis of cell proliferation and cell death, mice that had been injected in the left lateral cerebral ventricle 2 μ l of either 500 ng μ l⁻¹ EGF or 500 ng μ l⁻¹ EGF combined with 6 nmol μ l⁻¹ SKF-96365, were deeply anesthetized 6 hours post-injection and transcardially perfused with paraformaldehyde. Brains were removed and frontal sections, 40 μ m thick, were cut using a cryostat. Ki67 immunostaining, alone or along with SOX2, and TUNEL labeling were performed following denaturation during 20 minutes in sodium citrate buffer at 95°C, by using respectively a monoclonal mouse Ki67 antibody (1/250, Abcam, Cambridge, U.K.) and an in situ cell death detection kit (Sigma Aldrich).

Data Analysis

For in vitro experiments, data were derived from at least three independent experiments, each being performed with a culture derived from one animal ($N = 3$ experiments corresponds to three different mice). Cell numbers were counted on a Leica DMI6000 microscope. Percentages of GFAP, DCX, O4, nestin, or β III-tubulin immunoreactive cells were determined from counts in 15 fields of view in each coverslip with a 40 \times objective, by an observer blind to the assay (more than 250 cells were counted per coverslip).

Proliferative symmetric (SOX2+/SOX2+), asymmetric (SOX2+/SOX2-), and differentiative symmetric divisions (SOX2-/SOX2-) were counted with a spectral confocal FV-1000 station installed on an inverted microscope IX-81 (Olympus). Percentages of each type of cell pairs were determined from 20 to 60 cell pair counts in each coverslip with a 60 \times objective, by an observer blind to the assay.

For in vivo experiments, numbers of Ki67 and percentages of Ki67/SOX2 or BrdU/Ki67 labeled cells within the SVZ were determined for each mouse, on 13 brain sections collected at regular intervals from 1.42 mm anterior relative to Bregma to 0.1 mm posterior relative to Bregma (according to Franklin and Paxinos, The mouse brain in stereotaxic coordinates, 3rd Edition, 2008), with a 60 \times objective, by an observer blind to the assay.

Statistical significance of differences was examined by one-way analysis of variance followed by the post hoc Bonferroni test for multiple comparisons or by non-parametric Mann and Whitney test for comparison by pairs (Statview 5.00 software). Statistical significance level was set for p values < .05 and represented on the figures by: * for $p < .05$, ** for $p < .01$, *** for $p < .001$.

RESULTS

SVZ Cells Possess Functional SOC

SOC are mainly formed of Orai1 and/or TRPC1 calcium channels of the plasma membrane. STIM1, a sensor of calcium levels in the ER, activates SOC. To investigate if SVZ cells possess the machinery required for SOCE, we cultured SVZ cells derived from adult mice brains as neurospheres and analyzed on these cultures the presence of TRPC1, Orai1, and STIM1. RT-PCR (Fig. 1A) together with Western blotting (Fig. 1B) and immunostaining analysis (Fig. 1C–1E) showed that SVZ cells express TRPC1, Orai1, and STIM1. Possible physiological relevance of these in vitro data was assessed on mice brain sections and established that TRPC1, Orai1, and STIM1 are also found in SVZ cells in vivo (Fig. 1F–1H).

Next we determined whether SOC are functional in SVZ cells by measuring with calcium imaging their ability to support calcium entries in response to the depletion of ER calcium stores. To induce a decrease of the amount of free calcium in ER, we applied CPA, a blocker of calcium uptake in ER through the sarco-endoplasmic reticulum calcium-ATPase. We found that SVZ cells treated with CPA display a release of calcium in the cytoplasm (Fig. 2A; first peak), due to inhibition of calcium uptake and to a basal leak of calcium from ER. This passive store depletion is known to activate SOC at the plasma membrane. Although SOC open a few tenths of second after this calcium discharge, no calcium entry can occur as long as cells are maintained in a calcium-free buffer solution. Figure 2A illustrates that addition of calcium to the extracellular medium induces a calcium influx in SVZ cells (second peak, SOCE). For the quantitative analysis of SOCE, we focused on initial influx rates that are typical from SOCE while the maximal value of the second peak depends both on calcium entry through SOC and on processes that extrude calcium from cells. Thus, we measured the initial slopes from the calcium concentration traces obtained in Figure 2A. In addition, we used YM-58483 (10 μ mol l⁻¹) or SKF-96365 (40 μ mol l⁻¹) to block SOCE. Results reported in Figure 2B show that both YM-58483 and SKF-96365 drastically diminish SOCE induced by passive calcium depletion in SVZ cells.

Physiologically, SOCE are usually activated after stimulation of receptors coupled to PLC/IP3 pathway that promotes calcium release from the ER and secondary activation of STIM1. Figure 2C depicts that carbachol (10 μ mol l⁻¹), an agonist of cholinergic receptors, triggers in SVZ cells a biphasic intracellular rise of calcium formed of a rapid rising phase depending on calcium release from ER, followed by a sustained plateau. In cells placed in a calcium-free buffer solution, carbachol still induces the first calcium peak confirming that it is related to calcium release from internal stores, while the long-lasting plateau is lost (Fig. 2C), indicating that it depends on calcium entries. Moreover, addition of YM-58483 slightly decreases the maximum peak but markedly impairs the plateau phase (Fig. 2D), showing that SOCE supports in SVZ cells a long-lasting calcium response after ligand-evoked calcium release. In addition to ligand-induced calcium responses, SVZ cells can display an oscillatory calcium activity when maintained in their culture medium containing EGF and FGF (Fig. 2E). Known to stimulate specific cellular processes including cell proliferation, these calcium oscillations are abolished by SKF-96365 (Fig. 2F) or YM-58483 (not shown), suggesting that this oscillatory calcium signaling pattern also depends on SOC.

Altogether, our data demonstrate that SVZ cells possess SOC that support calcium entry in response to calcium store depletion induced by signals of the microenvironment.

SOC Regulate Proliferation of SVZ Cells Without Affecting Their Differentiation

First, we determined if SOC regulate SVZ cell proliferation. To this aim, we allowed SVZ cells to form neurospheres during 4 days and then added the SOC inhibitors SKF-96365 or YM-58483. Neurospheres were maintained in these conditions for five additional days, and then dissociated in order to count the cells by using the Trypan blue exclusion assay. Our data showed that both SKF-96365 (1 μ mol l⁻¹) and YM-58483 (5 μ mol l⁻¹) significantly reduce SVZ cell culture growth as

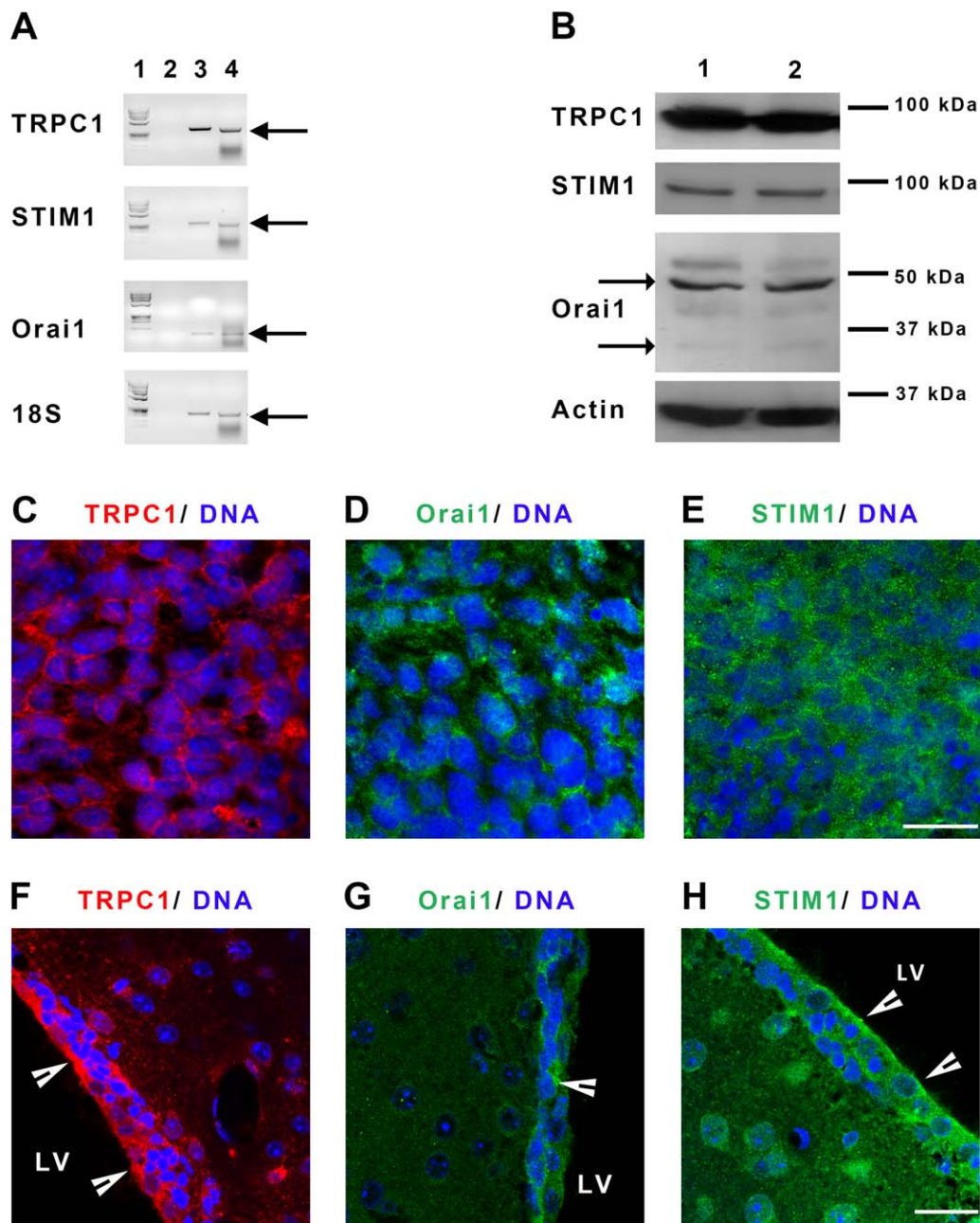


Figure 1. Subventricular zone (SVZ) cells express store-operated channels, TRPC1 and Orai1, and the endoplasmic reticulum calcium sensor STIM1. **(A):** RT-PCR detection of TRPC1, STIM1, and Orai1 transcripts in SVZ cells cultured as neurospheres (lane 3). Lane 1 corresponds to DNA molecular weight markers (PHI174 DNA/HaeIII). Lane 2 represents RT-PCR performed in the absence of reverse transcription (negative control). Lane 4 depicts RT-PCR products obtained using RNA from C2C12 myotubes known to express the transcripts (positive control). 18S ribosomal RNA was used as a positive control. Arrows point to the transcripts. **(B):** Western blot analysis of TRPC1, Orai1, and STIM1 proteins obtained from two different SVZ cell cultures (lanes 1 and 2). Molecular weights of the markers are given on the right of the figure. Arrows point to the two bands obtained for Orai1 that correspond to unglycosylated (35 kDa) and glycosylated (50 kDa) forms of Orai1. Micrographs representing immunostainings of TRPC1 (red, **C, F**), Orai1 (green, **D, G**) or STIM1 (green, **E, H**) on SVZ cell cultures (**C–E**) or on mice brain sections (**F–H**). Cell nuclei were labeled with TOPRO-3 (blue). Arrowheads indicate SVZ. Scale bars: 20 μm . Abbreviations: LV, lateral ventricle; STIM1, stromal interaction molecule 1; TRPC1, transient receptor potential canonical 1.

compared to their controls (Supporting Information Fig. S1). This decrease of SVZ cell numbers does not seem related to an increase of cell death, as neither SKF-96365 at $1 \mu\text{mol l}^{-1}$ nor YM-58483 at $5 \mu\text{mol l}^{-1}$ affect the proportions of dead (Supporting Information Fig. S1) or of apoptotic cells (Fig. 3A).

BrdU cell proliferation assay indicates that the reduction in SVZ cell number induced by SKF-96365 or YM-58483 is

due to an impairment of cell proliferation by SOC inhibitors. As shown in Figure 3B, SKF-96365 and YM-58483 dose-dependently decrease BrdU incorporation for concentrations ranging from 0.1 to $10 \mu\text{mol l}^{-1}$ and 1 to $20 \mu\text{mol l}^{-1}$, respectively.

SVZ cell cultures contain progenitors that have the ability to differentiate as neurons and as glial cells. Exposing SVZ cell

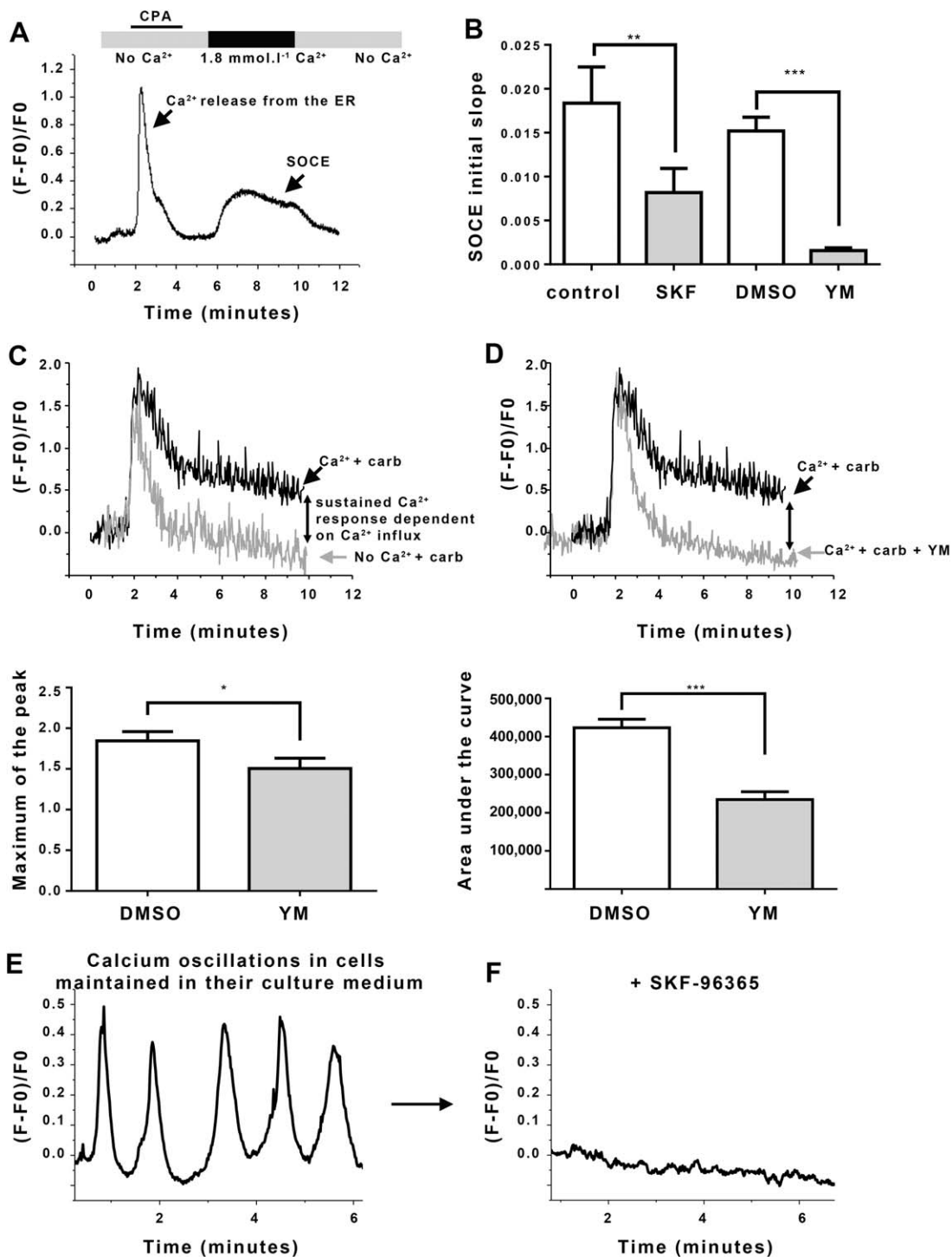


Figure 2. Living subventricular zone (SVZ) cells display SOCE. **(A):** A representative trace of SOCE recording in SVZ cells. SVZ cells loaded with Fluo8 were transferred to a zero calcium solution and to 15 $\mu\text{mol l}^{-1}$ CPA leading to the release of calcium from the ER (first peak). Replacement of zero calcium solution by a 1.8 mmol l^{-1} Ca²⁺ physiological buffer induced a calcium entry through SOC (second peak, SOCE). When cells were washed in a zero calcium solution, the fluorescent signal returned to initial level. **(B):** Bar graphs representing mean initial slope of the rising phase during the second peak. SOCE were recorded in control 1.8 mmol l^{-1} Ca²⁺ or with addition of SKF-96365 (SKF, 40 $\mu\text{mol l}^{-1}$), or YM-58483 (YM, 10 $\mu\text{mol l}^{-1}$) or DMSO. Data represented as means \pm SEM were obtained from recordings on at least 20 different cells per condition. **, $p = .0023$; ***, $p < .001$. **(C, D):** Representative traces of intracellular biphasic calcium signal in response to 10 $\mu\text{mol l}^{-1}$ carbachol (carb). The black trace was obtained in control conditions and displayed a sustained plateau phase due to SOC activation. The gray trace was obtained either (C) in an extracellular medium without calcium (No Ca²⁺) or in presence of 10 $\mu\text{mol l}^{-1}$ YM-58483 (D) and displayed a transient calcium signal without the plateau phase. Bar graphs represent the maximum peak of the first phase (left panel) and the area under curve of the complete response to carbachol (right panel) after carbachol stimulation in control conditions (DMSO) or with YM-58483. These data are represented as means \pm SEM and were obtained from recordings on at least 20 different cells per condition. *, $p = .0119$; ***, $p < .001$. **(E, F):** Representative traces of intracellular calcium oscillations recorded in SVZ cells maintained at 37°C, in their culture medium alone (E) or supplemented with 40 $\mu\text{mol l}^{-1}$ SKF-96365 (F). Abbreviations: CPA, cyclopiazonic acid; DMSO, diméthylsulfoxyde; ER, endoplasmic reticulum; SOCE, store-operated calcium entry.

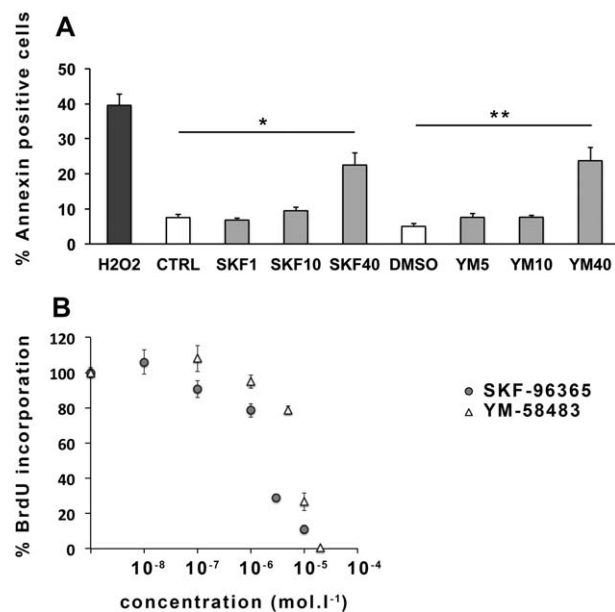


Figure 3. Pharmacological inhibition of store-operated channels inhibits subventricular zone (SVZ) cell proliferation. **(A):** Percentages of apoptotic Annexin V positive cells in SVZ cell cultures maintained for 24 hours in the presence of increasing concentrations of SKF-96365 or YM-58483 indicated on the figure in $\mu\text{mol l}^{-1}$ (e.g., SKF1 means SKF-96365 at $1 \mu\text{mol l}^{-1}$). Neither SKF-96365 nor YM-58483 induced apoptosis in SVZ cells up to $10 \mu\text{mol l}^{-1}$. Exposure of SVZ cells to SKF-96365 nor YM-58483 at $40 \mu\text{mol l}^{-1}$ for 24 hours increased the percentage of apoptotic cells from 6% in control condition to about 20% with SKF-96365 or YM-58483. H_2O_2 at 20mmol l^{-1} was used as a positive control. Data represent means \pm SEM from three independent experiments, each condition being assessed in duplicate per experiment. *, $p = .02$; **, $p = .0039$. **(B):** Percentages of BrdU incorporation in SVZ cells maintained for 24 hours in the presence of increasing concentrations of SKF-96365 or YM-58483. Data represent means \pm SEM from four independent experiments, each condition being assessed in quadruplicate per experiment. Abbreviations: BrdU, bromodeoxyuridine; DMSO, diméthylsulfoxyde.

cultures to SKF-96365 or YM-58483 affects neither percentages of cells in the neuronal lineage assessed by DCX immunostaining of neuroblasts (Fig. 4A, 4B) and by β III-tubulin labeling of neurons (Fig. 4C, 4D), nor those of GFAP expressing astrocytes (Fig. 4E, 4F), O4 labeled oligodendrocytes (Fig. 4G, 4H) or nestin immature cells (Supporting Information Fig. S2), suggesting that SOC are not involved in SVZ cell lineage orientation.

SOC Regulate Self-Renewal and Type of Division of SVZ NSC

SVZ neurospheres are formed of NSC but mainly of their progenies. As we found that SVZ cells possess functional SOC (Figs. 1, 2), we stained the nuclear epitope SOX2 to identify neural stem-like cells. Figure 5A–5C illustrate that SOX2-positive cells all express TRPC1 and STIM1 and part of them also express Orai1. Additional immunolabeling of combinations of NSC markers confirmed that NSC express SOC proteins (Supporting Information Fig. S3), suggesting that, within the different subpopulations of cells in SVZ cultures, NSC possess the machinery required for SOCE.

NSC are characterized *in vitro* by both their capacity to give rise to neurospheres and to self-renew when cultured in

the presence of mitogens. To address possible regulatory role of SOC on NSC activation, we exposed SVZ cultures to SKF-96365 or YM-58483 during 7 days and then, counted the primary neurospheres (Fig. 5D, SPHERE I), which reflect activated stem cells. Primary neurospheres contain both stem cells and their progenies. To quantify stem cells in the neurospheres and thus gain insight into the self-renewal process, we determined the number of cells capable of forming new neurospheres [44]. To this aim, we dissociated the cells of the primary neurospheres and plated them without the inhibitors to allow the formation of secondary neurospheres (Fig. 5D, SPHERE II). For this assay, we chose concentrations of SKF-96365 ($1 \mu\text{mol l}^{-1}$) and YM-58483 ($5 \mu\text{mol l}^{-1}$) that had only modest effects on SVZ cell proliferation (Fig. 3B) in order to let mitotic activity occur for the development of neurospheres. As shown in Figure 5E, both SKF-96365 and YM-58483 significantly decrease the number of primary neurospheres, which was confirmed with a neural colony formation assay (Supporting Information Fig. S4), suggesting that SOC are involved in NSC activation. When dissociated and plated without the inhibitors, primary neurospheres that had been exposed to SOC inhibitors for a week generate significantly less secondary neurospheres in comparison with control SVZ cultures (Fig. 5F), implying that SOC are also involved in NSC self-renewal.

The role of SOC in NSC was further explored through analysis of the type of cell division in SVZ cell cultures exposed to SOC inhibitors. To this aim, SVZ cells isolated from mice brains were plated for 18 hours with or without SKF-96365 ($1 \mu\text{mol l}^{-1}$) or YM-58483 ($5 \mu\text{mol l}^{-1}$) in culture medium containing low levels of EGF and FGF-2 to allow formation of cell pairs. The cultures were then labeled for the NSC marker SOX2 along with α -tubulin to accurately identify cell pairs (Fig. 5G). Three types of cell pairs corresponding to three types of divisions were distinguished: SOX2 positive-SOX2 positive pairs corresponding to symmetric proliferative divisions, SOX2 positive-SOX2 negative pairs corresponding to asymmetric divisions and SOX2 negative-SOX2 negative pairs corresponding to symmetric differentiative divisions. Results represented in Figure 5H show that both SKF-96365 and YM-58483 significantly diminish symmetric proliferative divisions for the benefit of asymmetric divisions, implying that SOC inhibition decreases the NSC population by shifting the type of division from symmetric proliferative to asymmetric.

Physiological Relevance of SOC Roles in NSC

Physiological relevance of the regulatory role of SOC on NSC population observed *in vitro* was then investigated *in vivo*. Immunostaining of mice brain sections shows that TRPC1, Orai1, and STIM1 are expressed by SOX2 positive NSC (Fig. 6A–6C). Additional immunodetection of NSC with either SOX2 and GFAP or nestin and GFAP (Fig. 6D) along with TRPC1, Orai1 or STIM1 shows that NSC express SOC proteins (Fig. 6E–6M).

Involvement of SOC on SVZ cell proliferation was then investigated by injecting *in vivo* a single dose of a solution containing EGF with either SKF-96365 or saline in the left lateral brain ventricle (Fig. 7A). Detection of proliferating cells by Ki67 immunostaining shows that SVZ from mice injected with EGF and SKF-96365 display significantly less Ki67 positive cells as compared to EGF-injected mice (173.0 ± 13.2 Ki67 positive cells per section in EGF+ SKF-96365 compared to 251.5 ± 29.8 in EGF condition), indicating that SOC regulate SVZ cell proliferation (Fig. 7B,

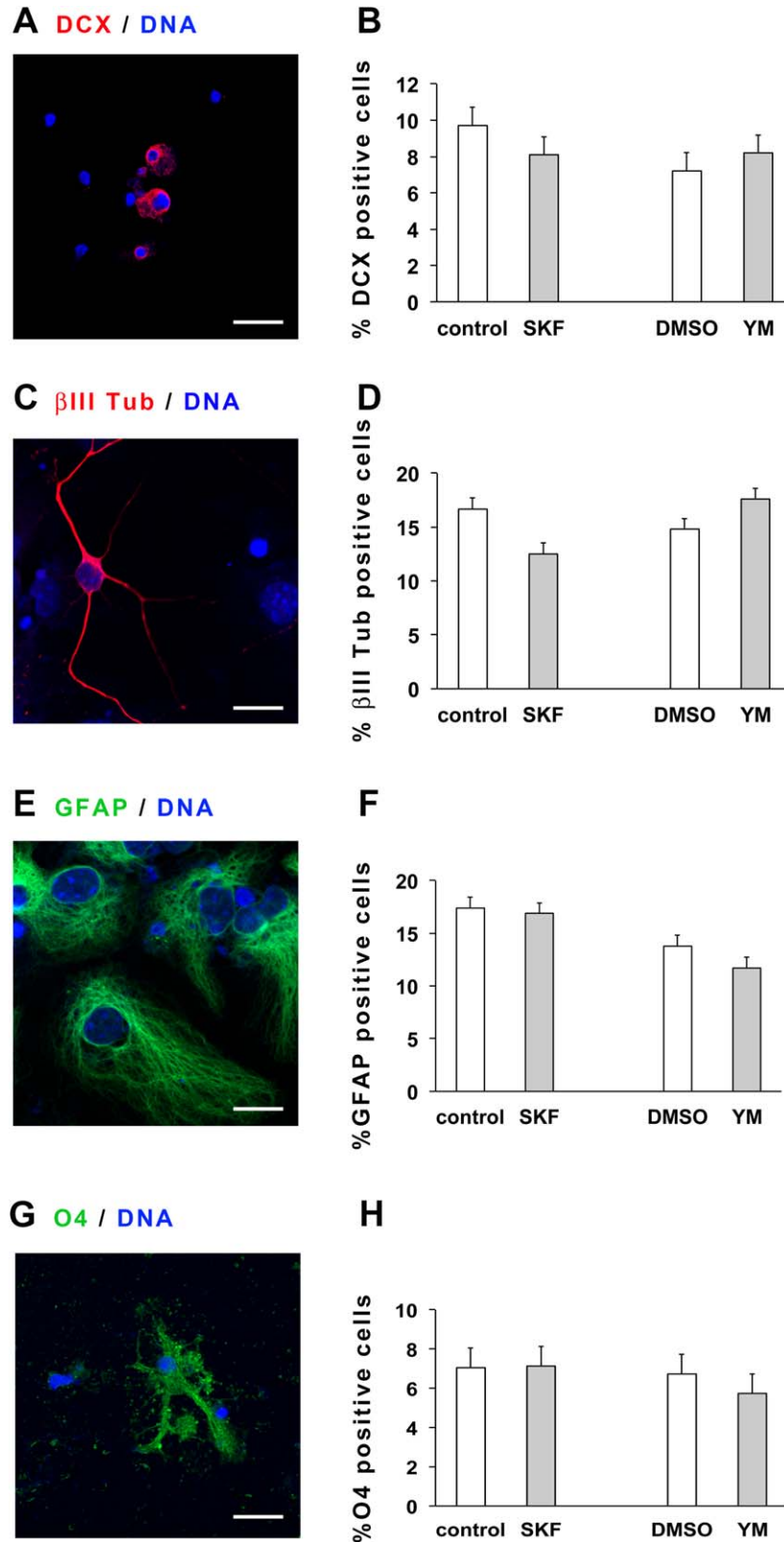


Figure 4. Pharmacological inhibition of store-operated channels does not affect subventricular zone (SVZ) cell differentiation. Micrographs (A, C, E, G) and illustrations of the proportions (B, D, F, H) of DCX expressing neuroblasts (red, A, B) or of β III-tubulin (β III Tub) expressing neurons (red, C, D) or of GFAP expressing astrocytes (green, E, F) or of O4 expressing oligodendrocytes (green G, H) in SVZ cell cultures maintained for 7 days in their culture medium without growth factor supplemented or not (control) with either $1 \mu\text{mol l}^{-1}$ SKF-96365 (SKF), or $5 \mu\text{mol l}^{-1}$ YM-58483 (YM) or DMSO (control of YM-58483). Cell nuclei were labeled with DAPI (blue). Scale bars: $15 \mu\text{m}$. Data represent means \pm SEM from three independent experiments, each condition being assessed in triplicate per experiment. Differences were significant neither between results from control versus SKF-96365 treated cultures ($p = .391$ for DCX experiments, $p = .149$ for β III-tubulin experiments, $p = .770$ for GFAP experiments, $p = .752$ for O4 experiments), nor between results from DMSO versus YM-58483 treated cultures ($p = .847$ for DCX experiments, $p = .110$ for β III-tubulin experiments, $p = .260$ for GFAP experiments, $p = .233$ for O4 experiments). Abbreviations: DCX, doublecortin; DMSO, dimethylsulfoxide.

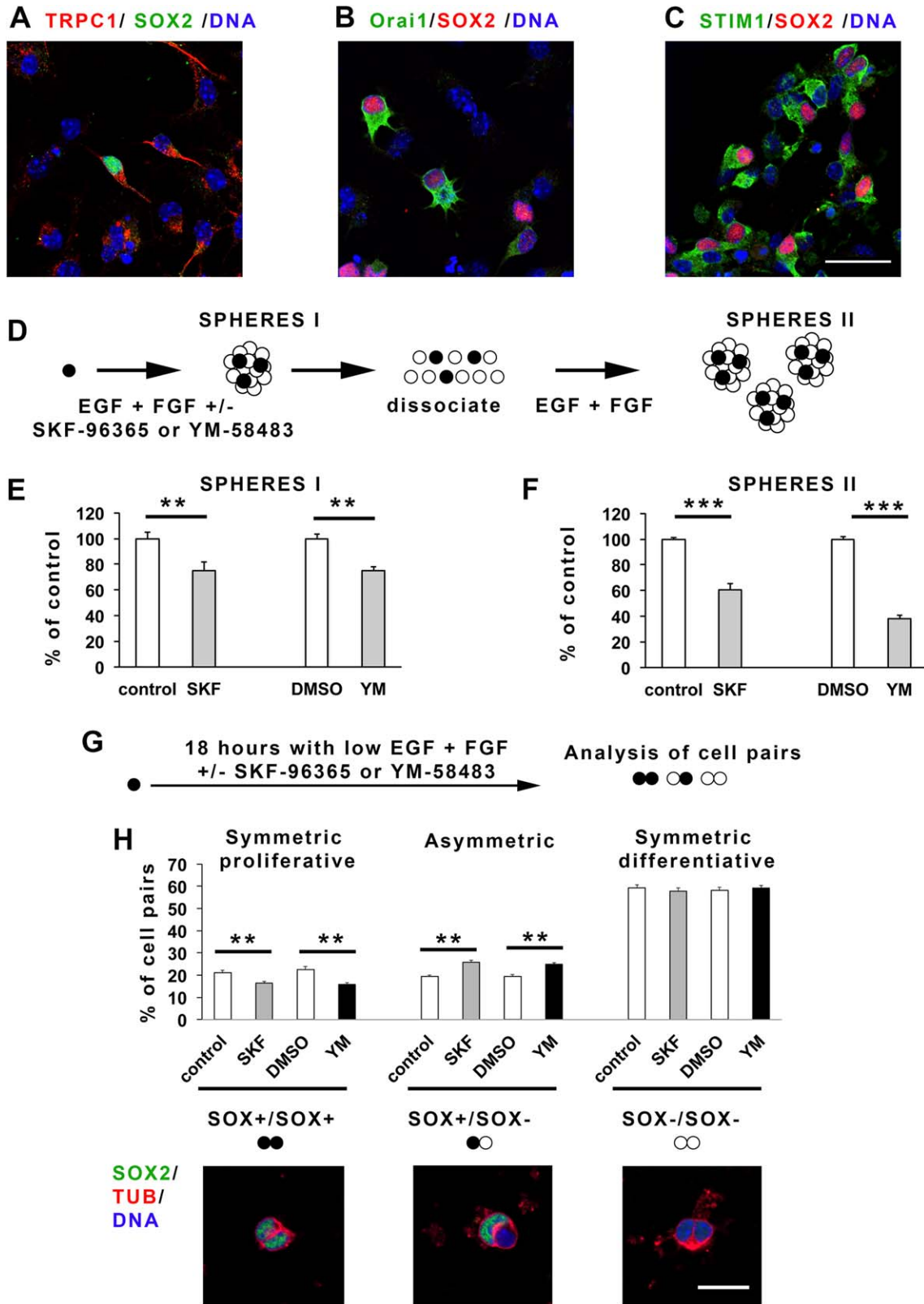


Figure 5. Pharmacological inhibition of store-operated channels inhibits subventricular zone (SVZ) stem cell self-renewal. Micrographs representing SVZ cells labeled with TRPC1 (red, **A**), Orai1 (green, **B**) or STIM1 (green, **C**) antibodies along with SOX2 antibody (A, green; B and C, red). Cell nuclei were labeled with TOPRO-3 (blue). Scale bar: 25 μm . **(D)**: Scheme of the neurosphere assay used to obtain data in **(E, F)**. Stem cells are represented as black-colored circles and progenitors as white-colored circles. Numbers of primary neurospheres (**E**, SPHERES I) or secondary neurospheres (**F**, SPHERES II) obtained following 1 week of culture with either 1 $\mu\text{mol l}^{-1}$ SKF-96365 or 5 $\mu\text{mol l}^{-1}$ YM-58483 or DMSO. Data are expressed as percent of control and represent means \pm SEM from eight independent experiments, each condition being assessed in triplicate per experiment. **, $p < .01$ ($p = .0055$ between control and SKF-96365; $p = .0014$ between DMSO and YM-58483), ***, $p < .001$. **(G)**: Scheme of the cell pair assay used to obtain data in **(H)**. **(H)** Percentages of symmetric proliferative (SOX2 positive/SOX2 positive), asymmetric (SOX2 positive/SOX2 negative), or symmetric differentiative (SOX2 negative/SOX2 negative) cell pairs in cultures maintained for 18 hours with either 1 $\mu\text{mol l}^{-1}$ SKF-96365, or 5 $\mu\text{mol l}^{-1}$ YM-58483, or DMSO. Examples of cell pairs are depicted. Scale bar: 15 μm . Data represent means \pm SEM from three independent experiments, each condition being assessed in triplicate per experiment. **, $p < .01$ (between control and SKF-96365, $p = .008$ for SOX2+/SOX2+ pairs and $p = .0013$ for SOX2+/SOX2- pairs; between DMSO and YM-58483, $p = .0035$ for SOX2+/SOX2+ pairs and $p = .0017$ for SOX2-/SOX2- pairs). Abbreviations: DMSO, dimethylsulfoxide; EGF, epidermal growth factor; STIM1, stromal interaction molecule 1; TRPC1, transient receptor potential canonical.

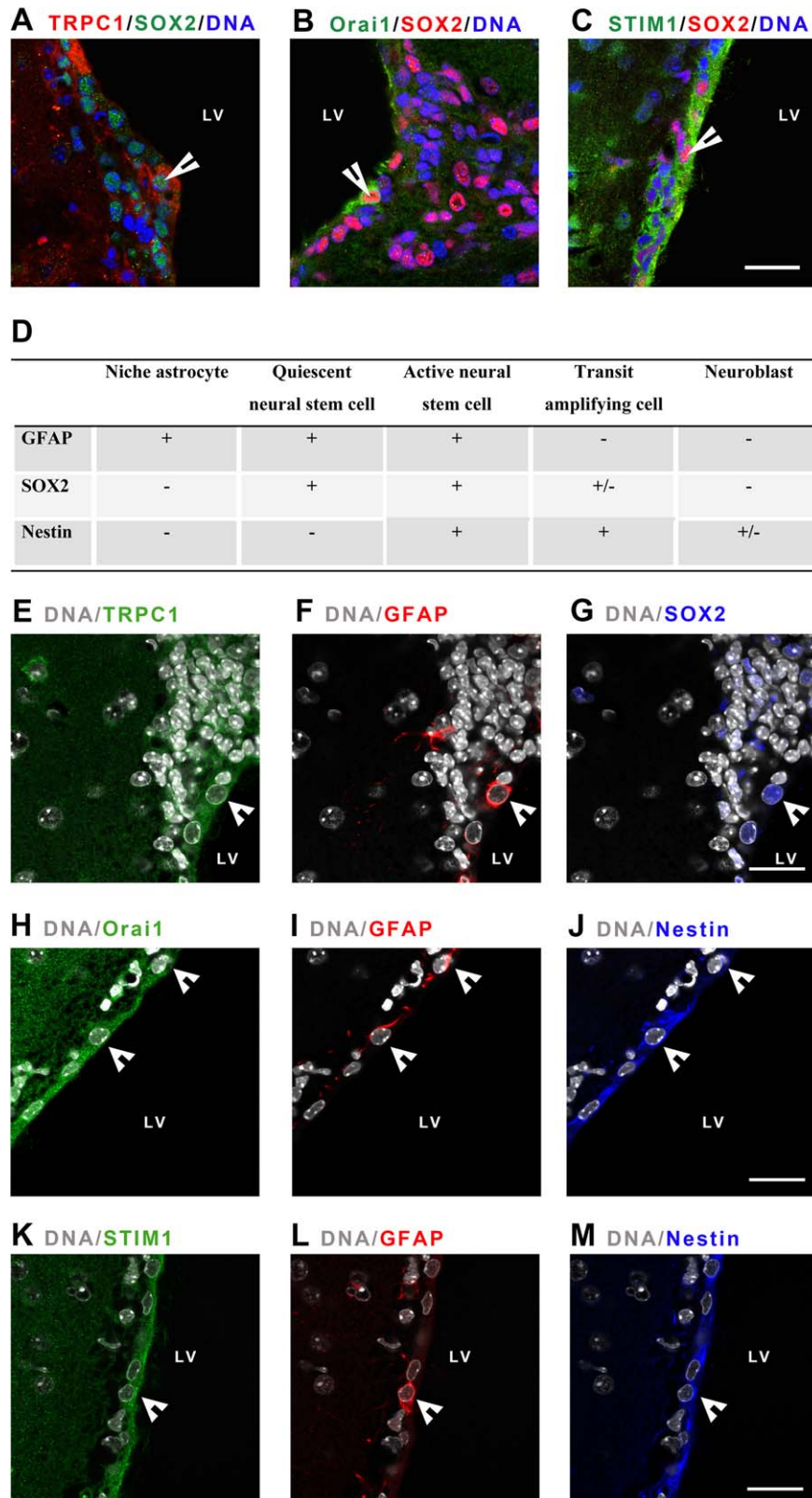


Figure 6. Store-operated channels are expressed by subventricular zone (SVZ) stem cells in vivo. Micrographs representing mice brain sections labeled with TRPC1 (red, **A**), Orai1 (green, **B**), or STIM1 (green, **C**) antibodies along with SOX2 antibody (A, green; B and C, red). Cell nuclei were stained with TOPRO-3 (blue). Arrowheads point to SVZ. The stem cell population was further characterized with combinations of either GFAP/SOX2 or GFAP/nestin immunostainings. Expression of the markers by the different cell populations of SVZ is given in (**D**). (**E–G**): Represent micrographs of the same region of a brain section immunolabeled with both TRPC1 (green, **E**), GFAP (red, **F**) and SOX2 (blue, **G**) antibodies along with DAPI to stain nuclei (gray). The arrow points to a cell that coexpresses TRPC1, GFAP, and SOX2. (**H–J**): Represent micrographs of the same region of a brain section immunolabeled with both Orai1 (green, **H**), GFAP (red, **I**) and nestin (blue, **J**) antibodies along with DAPI to stain nuclei (gray). The arrow points to a cell that coexpresses Orai1, GFAP, and nestin. (**K–M**): Represent micrographs of the same region of a brain section immunolabeled with both STIM1 (green, **K**), GFAP (red, **L**) and nestin (blue, **M**) antibodies along with DAPI to stain nuclei (gray). The arrow points to a cell that coexpresses STIM1, GFAP, and nestin. Scale bars: 20 μ m. Abbreviations: LV, lateral ventricle; STIM1, stromal interaction molecule 1; TRPC1, transient receptor potential canonical.

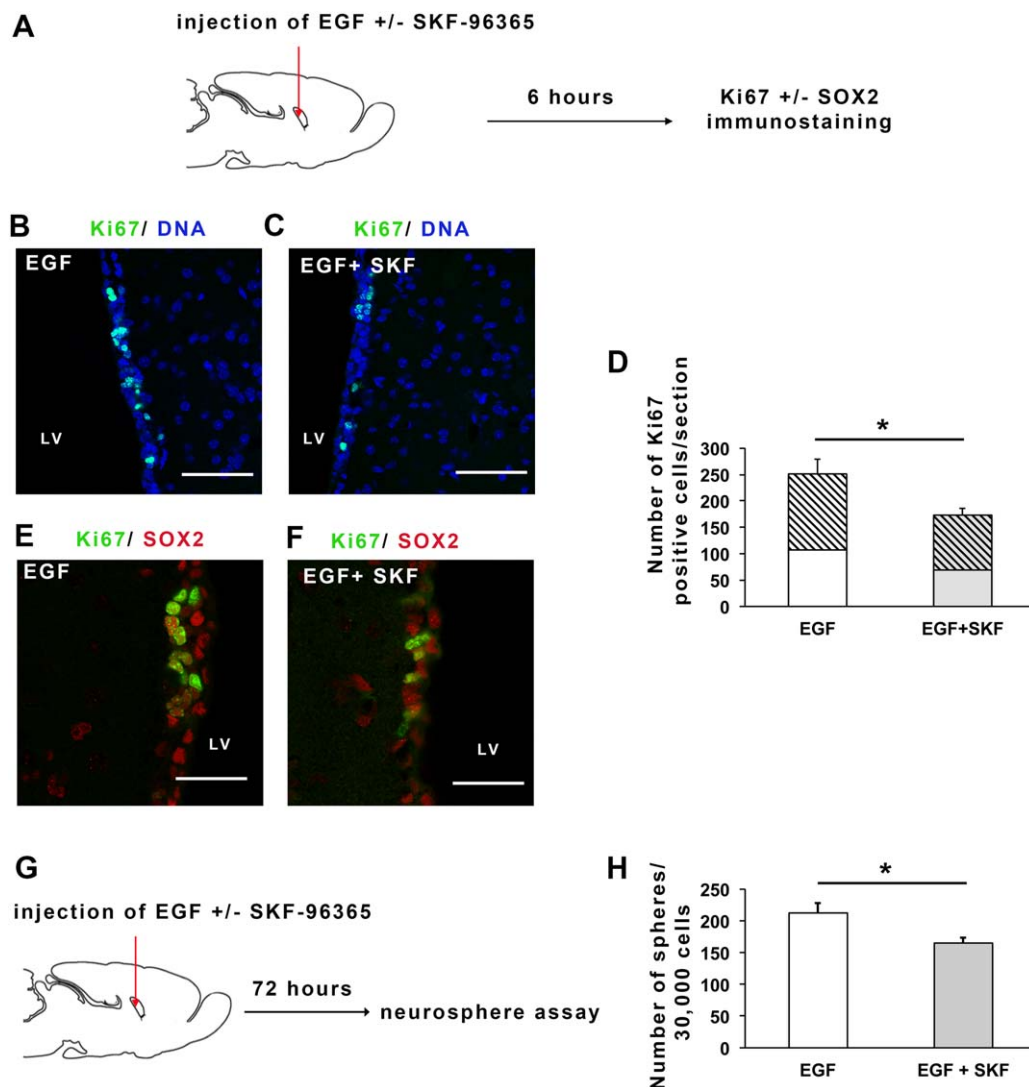


Figure 7. Store-operated channels regulate subventricular zone (SVZ) cell activity in vivo. **(A):** Scheme of the assay used for injections of EGF or EGF+SKF-96365 in a lateral ventricle of the brain to obtain data from **(C)** to **(F)**. Micrographs of Ki67 immunostaining (in green) of brain sections from mice injected with either EGF **(B)** or EGF combined with SKF-96365 **(C)**. Nuclei were labeled with TOPRO-3 (blue). Scale bars: 60 μ m. **(D)** Number of Ki67 positive cells per brain section in the SVZ of mice injected with either EGF or EGF combined with SKF-96365. Data represent means \pm SEM from six animals per condition. *, $p = .0161$. Micrographs of coimmunostaining of Ki67 (in green) and SOX2 (in red) of brain sections from mice injected with either EGF **(E)** or EGF combined with SKF-96365 **(F)**. Scale bars: 20 μ m. Percentages of SOX2 positive cells among Ki67 positive cells were determined in EGF and EGF+SKF-96365 injected brains (60% \pm 6.7% of SOX2 positive cells among Ki67 positive cells in EGF + SKF-96365 injected brains as compared to 57% \pm 5.4% in EGF injected brains, $p = .75$) and are represented as hatched lines on figure **(D)**. **(G)** Scheme of the assay used to obtain data represented in **(H)**. **(H)** Number of neurospheres obtained from SVZ microdissected from mice brain that had been injected with either EGF or EGF+ SKF-96365. Data represent means \pm SEM from seven animals per condition. *, $p = .0127$. Abbreviation: EGF, epidermal growth factor.

7C, 7D). Furthermore, TUNEL-labeling of brain sections shows that although SKF-96365 increases cell death in the SVZ (8.8 \pm 1.7 TUNEL positive cells per section in EGF+ SKF-96365 compared to 1.1 \pm 0.3 in EGF injected mice), the numbers of dead cells is much lower than the numbers of proliferating cells, suggesting that SKF-96365 major effect occurs through a reduction of cell proliferation. The proliferating cells were further analyzed for SOX2 expression (Fig. 7E, 7F). Injection of SKF-96365 along with EGF does not affect the percentage of SOX2 positive cells among the proliferating Ki67 positive cells. But, as the total number of proliferating cells decreases in the presence of SKF-96365, the number of SOX2 positive proliferating cells also diminishes in injected SKF-96365 brain (Fig. 7D hatched lines), suggesting that SKF-96365 reduces NSC population. In addition

to expressing SOX2, NSC possess an ability to generate neurospheres. Thus, we assessed if the in vivo injection of EGF with SKF-96365 could affect the SVZ NSC population that we characterized with the neurosphere assay (Fig. 7G). We found that SVZ cells derived from animals injected with SKF-96365 and EGF display a decreased capacity to form neurospheres as compared to EGF-injected animals (Fig. 7H), which suggests that SOC regulate the SVZ cell population with stem cell properties in vivo.

DISCUSSION

Using multiple approaches, our study shows that SVZ cells from the adult brain possess functional SOC and demonstrates that

calcium entries supported by these channels in addition to regulating cell proliferation, control NSC self-renewal by acting on the balance of symmetric versus asymmetric stem cell divisions. Thus, our study identifies SOC as key players for activation and expansion of the NSC population. As SOC trigger calcium entry in cells, our data not only provide support to the hypothesis of a major role of calcium in NSC that had been formulated on the basis of transcriptome analysis [22, 23], but also specify mechanisms underlying calcium effects in NSC.

In the process of this study, we observed that SVZ cells express TRPC1, Orai1, and their regulator STIM1 and we found that SVZ cells display SOCE, demonstrating that SVZ cells possess functional SOC. A previous study reported that SVZ cells express Orai1 and STIM1 [40]. Our study not only confirms the existence of SOCE in SVZ cells, but also shows that in addition to Orai1, SVZ cells also possess TRPC1, as do embryonic brain stem cells from which adult NSC derive [39, 45]. In addition to supporting calcium entries, SOC have been shown to activate voltage-gated channels in vascular cells [46]. A previous electrophysiological study [47] and our recordings (data not shown) indicate that SVZ stem cells are highly polarized and fail to produce action potentials. Thus, the effects of SOC on SVZ cells may mostly be related to calcium entries through SOC and subsequent signaling induced by these long-lasting calcium entries evoked by ligands of the microenvironment. Analysis of adult mice brain sections indicated that SOC molecular components are also present in vivo. Furthermore, we showed that SOX2 positive NSC express SOC, implying that NSC may be sensitive to calcium alterations and that those modifications in calcium signaling might affect NSC activities. Indeed, we found that exposing SVZ cells to SOC inhibitors reduce the capacity of NSC cells to activate and to self-renew, arguing for a major regulatory role of SOC and calcium signaling over NSC population.

Phenotypes observed following SOC inhibition or genetic alteration of Orai1 or TRPC1 assign a role for SOC in proliferation, survival, differentiation, or migration of various cell types including T cells, myoblasts, skin, or neural progenitors. During our study, we observed that pharmacological inhibition of SOC reduces SVZ cell proliferation as had been already shown for neural and other progenitors [28, 29, 38, 40, 48, 49]. In addition, we demonstrated that SOC inhibition decreases NSC self-renewal not only in vitro in SVZ cell cultures but also in vivo, following SOC inhibitor injection. This impairment of stem cell self-renewal caused by SOC inhibitors is correlated with a reduction in the proportion of symmetric proliferative for the benefit of asymmetric NSC division, resulting in an overall reduction of the NSC population. Our data thus provide evidence for the first time that SOC control stem cell population by acting on the fate of the daughter cells during division of stem cells. Although the mechanisms whereby SOC orient cell division remain hypothetical, it is interesting to mention that STIM1 and Orai1 can be localized to the cleavage furrow during cytokinesis [50]. These effects of SOC inhibition on cell proliferation and on self-renewal occur without any apparent change in cell differentiation, which is in accordance with previous studies [51].

Recently, it has been reported that brain tissue injury triggers calcium waves that activate NSC [51]. In our study, we observed that SOC support oscillatory calcium activities in SVZ cells maintained in their culture medium containing growth

factors, suggesting that SOC could be relevant targets for recruitment of NSC by brain lesions. Indeed, a shift from asymmetric to symmetric cell division of NSC, that in our study was regulated by SOC, had also been described to be impacted by brain injuries [52], arguing for a central role of SOC in NSC activation during brain tissue repair and would merit further investigation in future dedicated studies. In addition, we found that SOCE could support long-lasting calcium responses following stimulation by the cholinergic agonist carbachol. Our data showing cholinergic-induced SOCE and involvement of SOC in NSC proliferation and self-renewal are interesting to reconcile with the fact that the activity of cholinergic neurons controls proliferation in the SVZ [53] and that cholinergic agonists promote self-renewal of SVZ stem cells (Supporting Information Fig. S5). Thus, SOC, owing to their recruitment by a wide range of extracellular signals and because of their capacity to control stem cell proliferation and self-renewal, appear as critical actors for the adaptation of NSC activities to physiological signals, which would be interesting to deeply decipher in subsequent studies.

Genetic deletion of Orai1 or TRPC1 has been related to alterations in the immune system as well as to impairments in skin integrity, muscle function and regeneration or intestinal mucosa restitution after wounding [32, 33, 36, 37]. In the brain, ablation of TRPC1 or STIM1 in knockout mice results in memory deficiencies [54, 55]. Interestingly, adult neurogenesis has been implicated in learning and memory in both rodents and humans [56, 57] and learning defects induced by impairment of neurogenesis could be reversed by restoring neurogenesis [58–61]. The decreases of NSC proliferation and self-renewal induced by SOC inhibitors that we observed in vitro and in vivo after direct unilateral intracerebroventricular injection, suggest that SOCE could contribute to learning and memory not only by acting on synaptic remodeling of dendritic spines [62–65], but also by modulating NSC activities. In accordance, the Orai1 gene has been reported as one of the six candidate genes that could be responsible of the neurological phenotypes found in inherited microdeletion syndromes caused by a 445 kb chromosomal deletion [66]. Also, defective SOCE have been associated to severe brain disorders where stem cell dysfunctions have been reported like neurodegenerative Alzheimer's disease [67–69]. Conversely, increased SOC and STIM expression occurs in brain cancer cells that could arise from mutated NSC [70–73]. These data along with the demonstration we provide for a role of SOC in SVZ cell stemness regulation underline the importance of investigating SOC within the brain in physiological and pathological conditions and open new perspectives for further examining the physiological significance of the presence of SOC within the SVZ and other stem cell systems.

CONCLUSION

Our study assigns to SOC and store-operate calcium entries a key role in the regulation of NSC activation and self-renewal, and in the control of the balance of symmetric versus asymmetric cell divisions. As pathological alterations of calcium signaling lead to brain disorders wherein NSC dysfunctions have been described as leading events, a better understanding of

the mechanisms governing NSC activities is required for a further step toward brain repair.

ACKNOWLEDGMENTS

We are indebted to Anne Cantereau for her advices with confocal microscopy and Laetitia Cousin for technical assistance with brain section immunostaining and ELISA experiments. We thank Image UP microscopy core facilities and PREBIOS facilities for animal handling. This work was supported by La Ligue Contre le Cancer Grand Ouest Comités de la Vienne et des Deux Sèvres, Région Poitou-Charentes, FEDER HABISAN and ACI from Universities of Tours and of Poitiers. E. Terrié holds a Ph.D. fellowship from Région Nouvelle-Aquitaine.

AUTHOR CONTRIBUTIONS

F.D.: collection, assembly, analysis and interpretation of data on cell differentiation, cell division; E.T.: collection, assembly

and interpretation of data on cell differentiation, cell death, neural colony forming assay and on calcium imaging; P.A.: collection, assembly, analysis and interpretation of in vivo data, manuscript writing; T.H.: design, analysis and interpretation of Western blot data; C.M.: collection, assembly, analysis and interpretation of RT-PCR data; P.B.: analysis and interpretation of RT-PCR data, manuscript writing; B.C.: conception and design, collection, assembly, analysis and interpretation of calcium imaging data, manuscript writing; V.C.: conception and design, financial support, collection, assembly, analysis and interpretation of data, manuscript writing; F.D., E.T., P.A., T.H., C.M., P.B., B.C., and V.C.: final approval of manuscript.

DISCLOSURE OF POTENTIAL CONFLICTS OF INTEREST

The authors indicated no potential conflicts of interest.

REFERENCES

- Lim DA, Alvarez-Buylla A. The adult ventricular-subventricular zone (V-SVZ) and olfactory bulb (OB) neurogenesis. *Cold Spring Harb Perspect Biol* 2016;8:a018820.
- Lois C, Alvarez-Buylla A. Long-distance neuronal migration in the adult mammalian brain. *Science* 1994;264:1145–1148.
- Sailor KA, Schinder AF, Lledo P-M. Adult neurogenesis beyond the niche: Its potential for driving brain plasticity. *Curr Opin Neurobiol* 2017;42:111–117.
- Menn B, Garcia-Verdugo JM, Yaschine C et al. Origin of oligodendrocytes in the subventricular zone of the adult brain. *J Neurosci* 2006;26:7907–7918.
- Gonzalez-Perez O, Romero-Rodriguez R, Soriano-Navarro M et al. Epidermal growth factor induces the progeny of subventricular zone type B cells to migrate and differentiate into oligodendrocytes. *STEM CELLS* 2009;27:2032–2043.
- Nait-Oumesmar B, Picard-Riera N, Kerninon C et al. Activation of the subventricular zone in multiple sclerosis: Evidence for early glial progenitors. *Proc Natl Acad Sci USA* 2007;104:4694–4699.
- Jin K, Minami M, Lan JQ et al. Neurogenesis in dentate subgranular zone and rostral subventricular zone after focal cerebral ischemia in the rat. *Proc Natl Acad Sci USA* 2001;98:4710–4715.
- Yamashita T, Ninomiya M, Hernández Acosta P et al. Subventricular zone-derived neuroblasts migrate and differentiate into mature neurons in the post-stroke adult striatum. *J Neurosci* 2006;26:6627–6636.
- Wang X, Mao X, Xie L et al. Conditional depletion of neurogenesis inhibits long-term recovery after experimental stroke in mice. *PLoS One* 2012;7:e38932.
- Xing YL, Röth PT, Stratton JAS et al. Adult neural precursor cells from the subventricular zone contribute significantly to oligodendrocyte regeneration and remyelination. *J Neurosci* 2014;34:14128–14146.
- Sanai N, Tramontin AD, Quiñones-Hinojosa A et al. Unique astrocyte ribbon in adult human brain contains neural stem cells but lacks chain migration. *Nature* 2004;427:740–744.
- Ayuso-Sacido A, Roy NS, Schwartz TH et al. Long-term expansion of adult human brain subventricular zone precursors. *Neurosurgery* 2008;62:223–229; discussion 229–231.
- Westerlund U, Svensson M, Moe MC et al. Endoscopically harvested stem cells: A putative method in future autotransplantation. *Neurosurgery* 2005;57:779–784; discussion 779–784.
- Jin K, Wang X, Xie L et al. Evidence for stroke-induced neurogenesis in the human brain. *Proc Natl Acad Sci USA* 2006;103:13198–13202.
- Martí-Fàbregas J, Romaguera-Ros M, Gómez-Pinedo U et al. Proliferation in the human ipsilateral subventricular zone after ischemic stroke. *Neurology* 2010;74:357–365.
- Bergmann O, Liebl J, Bernard S et al. The age of olfactory bulb neurons in humans. *Neuron* 2012;74:634–639.
- Ernst A, Alkass K, Bernard S et al. Neurogenesis in the striatum of the adult human brain. *Cell* 2014;156:1072–1083.
- Curtis MA, Kam M, Nannmark U et al. Human neuroblasts migrate to the olfactory bulb via a lateral ventricular extension. *Science* 2007;315:1243–1249.
- Nogueira AB, Sogayar MC, Colquhoun A et al. Existence of a potential neurogenic system in the adult human brain. *J Transl Med* 2014;12:75.
- Sanai N, Nguyen T, Ithrie RA et al. Corridors of migrating neurons in the human brain and their decline during infancy. *Nature* 2011;478:382–386.
- Macas J, Nern C, Plate KH et al. Increased generation of neuronal progenitors after ischemic injury in the aged adult human forebrain. *J Neurosci* 2006;26:13114–13119.
- Beckervordersandforth R, Tripathi P, Ninkovic J et al. In vivo fate mapping and expression analysis reveals molecular hallmarks of prospectively isolated adult neural stem cells. *Cell Stem Cell* 2010;7:744–758.
- Sandberg CJ, Vik-Mo EO, Behnan J et al. Transcriptional profiling of adult neural stem-like cells from the human brain. *PLoS One* 2014;9:e114739.
- Berridge M, Lipp P, Bootman M. Calcium signalling. *Curr Biol* 1999;9:R157–R159.
- Prakriya M, Lewis RS. Store-operated calcium channels. *Physiol Rev* 2015;95:1383–1436.
- Albarran L, Lopez JJ, Salido GM et al. Historical overview of store-operated Ca(2+) entry. *Adv Exp Med Biol* 2016;898:3–24.
- Louis M, Zanou N, Van Schoor M et al. TRPC1 regulates skeletal myoblast migration and differentiation. *J Cell Sci* 2008;121:3951–3959.
- Kuang C, Yu Y, Wang K et al. Knockdown of transient receptor potential canonical-1 reduces the proliferation and migration of endothelial progenitor cells. *Stem Cells Dev* 2012;21:487–496.
- Dragoni S, Laforenza U, Bonetti E et al. Vascular endothelial growth factor stimulates endothelial colony forming cells proliferation and tubulogenesis by inducing oscillations in intracellular Ca2+ concentration. *STEM CELLS* 2011;29:1898–1907.
- Darbellay B, Arnaudeau S, König S et al. STIM1- and Orai1-dependent store-operated calcium entry regulates human myoblast differentiation. *J Biol Chem* 2009;284:5370–5380.
- Peng H, Hao Y, Mousawi F et al. Purinergic and store-operated Ca(2+) signaling mechanisms in mesenchymal stem cells and their roles in ATP-induced stimulation of cell migration. *STEM CELLS* 2016;34:2102–2114.
- Feske S, Gwack Y, Prakriya M et al. A mutation in Orai1 causes immune deficiency by abrogating CRAC channel function. *Nature* 2006;441:179–185.
- Vandenbergh M, Raphaël M, Lehen'kyi V et al. Orai1 calcium channel orchestrates skin homeostasis. *Proc Natl Acad Sci USA* 2013;110:E4839–E4848.
- McCarl C-A, Picard C, Khalil S et al. Orai1 deficiency and lack of store-operated Ca2+ entry cause immunodeficiency, myopathy, and ectodermal dysplasia. *J Allergy Clin Immunol* 2009;124:1311–1318.e7.

- 35 Gwack Y, Srikanth S, Oh-Hora M et al. Hair loss and defective T- and B-cell function in mice lacking Orai1. *Mol Cell Biol* 2008;28:5209–5222.
- 36 Rao JN, Rathor N, Zou T et al. STIM1 translocation to the plasma membrane enhances intestinal epithelial restitution by inducing TRPC1-mediated Ca²⁺ signaling after wounding. *Am J Physiol Cell Physiol* 2010;299:C579–C588.
- 37 Zanou N, Schakman O, Louis P et al. Trpc1 ion channel modulates phosphatidylinositol 3-kinase/Akt pathway during myoblast differentiation and muscle regeneration. *J Biol Chem* 2012;287:14524–14534.
- 38 Li M, Chen C, Zhou Z et al. A TRPC1-mediated increase in store-operated Ca²⁺ entry is required for the proliferation of adult hippocampal neural progenitor cells. *Cell Calcium* 2012;51:486–496.
- 39 Fiorio Pla A, Maric D, Brazer S-C et al. Canonical transient receptor potential 1 plays a role in basic fibroblast growth factor (bFGF)/FGF receptor-1-induced Ca²⁺ entry and embryonic rat neural stem cell proliferation. *J Neurosci* 2005;25:2687–2701.
- 40 Somasundaram A, Shum AK, McBride HJ et al. Store-operated CRAC channels regulate gene expression and proliferation in neural progenitor cells. *J Neurosci* 2014;34:9107–9123.
- 41 Ginisty A, Gély-Pernot A, Abamrane L et al. Evidence for a subventricular zone neural stem cell phagocytic activity stimulated by the vitamin K-dependent factor protein S. *STEM CELLS* 2015;33:515–525.
- 42 Kiviluoto S, Decuyper J-P, De Smedt H et al. STIM1 as a key regulator for Ca²⁺ homeostasis in skeletal-muscle development and function. *Skelet Muscle* 2011;1:16.
- 43 Azari H, Louis SA, Shariffar S et al. Neural-colony forming cell assay: An assay to discriminate bona fide neural stem cells from neural progenitor cells. *J Vis Exp* 2011;49:e2639.
- 44 Hamilton LK, Dufresne M, Joppé SE et al. Aberrant lipid metabolism in the forebrain niche suppresses adult neural stem cell proliferation in an animal model of Alzheimer's disease. *Cell Stem Cell* 2015;17:397–411.
- 45 Merkle FT, Tramontin AD, García-Verdugo JM et al. Radial glia give rise to adult neural stem cells in the subventricular zone. *Proc Natl Acad Sci USA* 2004;101:17528–17532.
- 46 Ávila-Medina J, Calderón-Sánchez E, González-Rodríguez P et al. Orai1 and TRPC1 proteins co-localize with Ca_v1.2 channels to form a signal complex in vascular smooth muscle cells. *J Biol Chem* 2016;291:21148–21159.
- 47 Lai B, Mao XO, Xie L et al. Electrophysiological properties of subventricular zone cells in adult mouse brain. *Brain Res* 2010;1340:96–105.
- 48 Wong C-K, So W-Y, Law S-K et al. Estrogen controls embryonic stem cell proliferation via store-operated calcium entry and the nuclear factor of activated T-cells (NFAT). *J Cell Physiol* 2012;227:2519–2530.
- 49 Chen H-C, Wang C-H, Shih C-P et al. TRPC1 is required for survival and proliferation of cochlear spiral ganglion stem/progenitor cells. *Int J Pediatr Otorhinolaryngol* 2015;79:2290–2294.
- 50 Chan CM, Aw JTM, Webb SE et al. SOCE proteins, STIM1 and Orai1, are localized to the cleavage furrow during cytokinesis of the first and second cell division cycles in zebrafish embryos. *Zygote* 2016;24:880–889.
- 51 Kraft A, Jubal ER, von Laer R et al. Astrocytic calcium waves signal brain injury to neural stem and progenitor cells. *Stem Cell Reports* 2017;8:701–714.
- 52 Zhang R, Zhang Z, Zhang C et al. Stroke transiently increases subventricular zone cell division from asymmetric to symmetric and increases neuronal differentiation in the adult rat. *J Neurosci* 2004;24:5810–5815.
- 53 Paez-Gonzalez P, Asrican B, Rodriguez E et al. Identification of distinct ChAT⁺ neurons and activity-dependent control of postnatal SVZ neurogenesis. *Nat Neurosci* 2014;17:934–942.
- 54 Garcia-Alvarez G, Shetty MS, Lu B et al. Impaired spatial memory and enhanced long-term potentiation in mice with forebrain-specific ablation of the Stim genes. *Front Behav Neurosci* 2015;9:180.
- 55 Xing R, Zhang Y, Xu H et al. Spatial memory impairment by TRPC1 depletion is ameliorated by environmental enrichment. *Oncotarget* 2016;7:27855–27873.
- 56 Gonçalves JT, Schafer ST, Gage FH. Adult neurogenesis in the hippocampus: From stem cells to behavior. *Cell* 2016;167:897–914.
- 57 Coras R, Siebzehnrubl FA, Pauli E et al. Low proliferation and differentiation capacities of adult hippocampal stem cells correlate with memory dysfunction in humans. *Brain J Neurol* 2010;133:3359–3372.
- 58 Alonso M, Lepousez G, Sebastien W et al. Activation of adult-born neurons facilitates learning and memory. *Nat Neurosci* 2012;15:897–904.
- 59 Morales-Garcia JA, Echeverry-Alzate V, Alonso-Gil S et al. Phosphodiesterase7 inhibition activates adult neurogenesis in hippocampus and subventricular zone in vitro and in vivo. *STEM CELLS* 2017;35:458–472.
- 60 Arruda-Carvalho M, Akers KG, Guskjolen A et al. Posttraining ablation of adult-generated olfactory granule cells degrades odor-reward memories. *J Neurosci* 2014;34:15793–15803.
- 61 Wang JM, Singh C, Liu L et al. Allopregnanolone reverses neurogenic and cognitive deficits in mouse model of Alzheimer's disease. *Proc Natl Acad Sci USA* 2010;107:6498–6503.
- 62 Dhar M, Wayman GA, Zhu M et al. Leptin-induced spine formation requires TrpC channels and the CaM kinase cascade in the hippocampus. *J Neurosci* 2014;34:10022–10033.
- 63 Moccia F, Zuccolo E, Soda T et al. Stim and Orai proteins in neuronal Ca(2+) signaling and excitability. *Front Cell Neurosci* 2015;9:153.
- 64 Tshuva RY, Korkotian E, Segal M. Orai1-dependent synaptic plasticity in rat hippocampal neurons. *Neurobiol Learn Mem* 2017;140:1–10.
- 65 Korkotian E, Oni-Biton E, Segal M. The role of the store-operated calcium entry channel Orai1 in cultured rat hippocampal synapse formation and plasticity. *J Physiol* 2017;595:125–140.
- 66 Labonne DJ, Lee K-H, Iwase S et al. An atypical 12q24.31 microdeletion implicates six genes including a histone demethylase KDM2B and a histone methyltransferase SETD1B in syndromic intellectual disability. *Hum Genet* 2016;135:757–771.
- 67 Vigont V, Kolobkova Y, Skopin A et al. Both Orai1 and TRPC1 are involved in excessive store-operated calcium entry in striatal neurons expressing mutant huntingtin exon 1. *Front Physiol* 2015;6:337.
- 68 Tong BC-K, Lee CS-K, Cheng W-H et al. Familial Alzheimer's disease-associated presenilin 1 mutants promote γ -secretase cleavage of STIM1 to impair store-operated Ca²⁺ entry. *Sci Signal* 2016;9:ra89.
- 69 Demars M, Hu Y-S, Gadadhar A et al. Impaired neurogenesis is an early event in the etiology of familial Alzheimer's disease in transgenic mice. *J Neurosci Res* 2010;88:2103–2117.
- 70 Motiani RK, Hyzinski-García MC, Zhang X et al. STIM1 and Orai1 mediate CRAC channel activity and are essential for human glioblastoma invasion. *Pflugers Arch* 2013;465:1249–1260.
- 71 Marumoto T, Tashiro A, Friedmann-Morvinski D et al. Development of a novel mouse glioma model using lentiviral vectors. *Nat Med* 2009;15:110–116.
- 72 Barami K, Sloan AE, Rojiani A et al. Relationship of gliomas to the ventricular walls. *J Clin Neurosci* 2009;16:195–201.
- 73 Jiang Y, Marinescu VD, Xie Y et al. Glioblastoma cell malignancy and drug sensitivity are affected by the cell of origin. *Cell Rep* 2017;18:977–990.



See www.StemCells.com for supporting information available online.